RSC Advances

REVIEW

View Article Online
View Journal | View Issue

Cite this: *RSC Adv.*, 2023, **13**, 16693

Research status of polysiloxane-based piezoresistive flexible human electronic sensors

Xiaoyu Zhang,†[a] Ning Li,†*[a] Guorui Wang,[a] Chi Zhang,[a] Yu Zhang,[a] Fanglei Zeng,[a] Hailong Liu,[b] Gang Yi*[b] and Zhongwei Wang*[c]

Flexible human body electronic sensor is a multifunctional electronic device with flexibility, extensibility, and responsiveness. Piezoresistive flexible human body electronic sensor has attracted the extensive attention of researchers because of its simple preparation process, high detection sensitivity, wide detection range, and low power consumption. However, the wearability and affinity to the human body of traditional flexible human electronic sensors are poor, while polysiloxane materials can be mixed with other electronic materials and have good affinity toward the human body. Therefore, polysiloxane materials have become the first choice of flexible matrixes. In this study, the research progress and preparation methods of piezoresistive flexible human electronic sensors based on polysiloxane materials in recent years are summarized, the challenges faced in the development of piezoresistive flexible human electronic sensors are analyzed, and the future research directions are prospected.

Received 16th May 2023
Accepted 21st May 2023

DOI: 10.1039/d3ra03258b

rsc.li/rsc-advances

1 Introduction

In recent years, with the continuous progress of science and technology, sensing technology and electronic materials have developed rapidly. As a combination of two advanced technologies, flexible electronic sensors have attracted extensive attention of researchers. Traditional sensors mostly use rigid materials as the matrix, such as silicon-boron carbon nitride (SiBCN) and functionalized soda-lime glass.[1–4] Shao[1] *et al.* prepared a SiBCN ceramic pressure sensor with extremely high linearity, sensitivity, accuracy, as well as a high-pressure sensing

[a]*Jiangsu Collaborative Innovation Center for Photovoltaic Science and Engineering, Jiangsu Province Cultivation Base for State Key Laboratory of Photovoltaic Science and Technology, Jiangsu Province Key Laboratory of Environmentally Friendly Polymer Materials, School of Materials Science and Engineering, Changzhou University, Changzhou 213164, China. E-mail: czlin20201116@163.com*

[b]*Shandong Dongyue Silicone Material Co. ,Ltd., Zibo 256401, China. E-mail: yigang009@163.com*

[c]*College of Materials Science and Engineering, Shandong University of Science and Technology, Qingdao 266590, China. E-mail: wangzhongwei@fusilinchem.com*

† These authors contributed to this work equally.

Xiaoyu Zhang received his bachelor degree in polymer materials science and engineering from Changzhou University (CCZU) in 2021. Under the guidance of Professor Ning Li, he continues to study for a master degree. His main research direction is the synthesis and application of silicone materials.

Prof Ning Li received his PhD degree in Polymer Material Science and Technology at Harbin Institute of Technology (HIT) in 2017. His main research interests include the synthesis and applications of functional polysiloxane, polyurethane, and fluoropolymers. His research team has successfully developed more than twenty novel products under his direction, including polysiloxane or fluorinated coatings, polyurethane elastomer and special adhesives. He is also a member of the Editorial Boards of Chemical research progress, Polymers, and Journal of Research progress in aviation bonding materials.

range (0–10 MPa). The sensor has promising application prospects in pressure measurement in extreme environments.

However, rigid materials have poor affinity to the human body due to their high hardness and poor practicability. To meet the practical needs in real life, the flexible sensor based on polymer material[5–10] solves this problem well. Flexible sensors have softness, stretchability, and excellent mechanical properties.[11,12] They can be attached to the surface of human skin to capture physiological signals, such as joint motion, heartbeat, and vocal cord vibration, and then convert physiological signals into electrical signals to transmit information.[13–16] Therefore, flexible sensors have broad application prospects in human motion monitoring, health management, biomedicine, electronic robots, and other fields.[17,18]

Piezoresistive flexible sensors have the advantages of large measurement range, short response time, and high sensitivity. In addition, compared to other types of sensors, piezoresistive sensors have lower preparation costs and stronger anti-interference capabilities.[19–23] At present, thermoplastic polyurethane (TPU),[10] polyimide (PI),[11] polyethylene terephthalate (PET),[12] flexible paper,[24–28] flexible fabric,[29] polydimethylsiloxane (PDMS),[13] and modified polysiloxane elastomers[30] are commonly used as flexible substrates of flexible sensors. Among them, polysiloxane materials have the advantages of softness,[13,14] chemical stability,[15] high thermal stability,[16,17] and good hydrophobicity.[9,18] Moreover, unlike most flexible matrixes, polysiloxane materials have the characteristics of being mixed with other electronic materials and have good affinity toward the human body;[12,18] thus, polysiloxane materials are the first choice for flexible matrixes.

Based on different substrate materials, conductive fillers, and flexible sensor preparation processes, this study mainly introduces the piezoresistive flexible human electronic sensors with various polysiloxanes as flexible substrates in recent years, lists the technical challenges faced by this type of sensors at present, and looks forward to its development direction (Fig. 1).

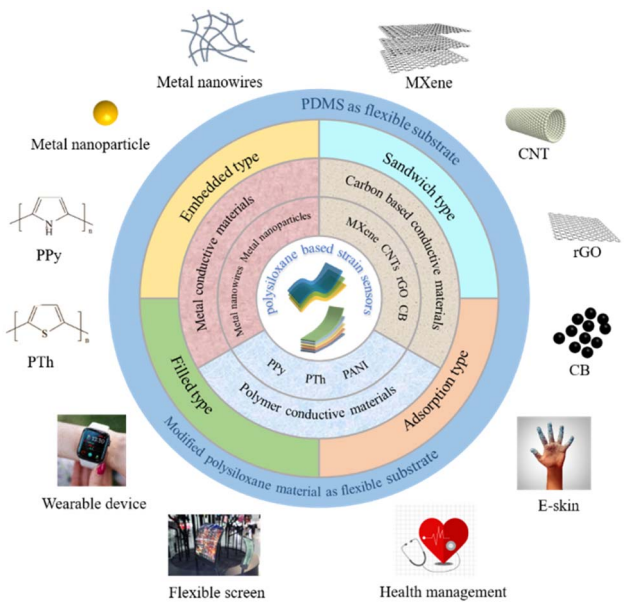

Fig. 1 Overview of several typical polysiloxane-based piezoresistive flexible human electronic sensors.

2 Sensing mechanism of piezoresistive flexible sensor

Piezoresistive flexible sensors have the advantages of simple preparation process,[31–34] high sensitivity,[35–39] large detection range,[40–49] and wide application.[50,51] It is an important direction for the development of flexible electronic sensors. The piezoresistive flexible sensor is composed of a flexible substrate and conductive fillers. Its sensing principle is to convert the mechanical signals caused by human motion,[52–59] heartbeat,[60–65] vocal cord vibration,[66–69] *etc.*, into changes in resistance,[70] resulting in changes in the size of the current, which is then detected by the sensor, as shown in Fig. 2(a).

There are three kinds of sensing mechanisms to explore the resistance flexible sensor from the microscopic point of view, which are crack propagation, tunneling effect, and disconnection mechanism. Crack propagation[72] means that when the flexible sensor is stretched or extruded to produce deformation, the conductive network composed of conductive fillers will have microcracks, which will reduce the conductive path and then increase the resistance, and then the deformation will recover, the microcracks will heal again and then the resistance of the sensor will recover. Yang[73] *et al.* designed a flexible sensor based on a new sandwich structure, blended PDMS, and polyvinylidene fluoride (PVDF) to prepare a highly elastic electrospun film and pumped silver nanowires (AgNWs) into the electrospun film to prepare a flexible sensor with a sandwich structure. The author's team observed that the microcrack structure was the main reason for the high sensitivity of the sensor, and the gauge factor (GF) of the sensor was as high as 3058.

The tunneling effect[74,75] means that according to the theory of quantum mechanics, microscopic particles have wave particle duality; thus, microscopic particles have the possibility to pass through the "wall" they could not pass through, thus forming a conductive path. When the flexible sensor deforms,

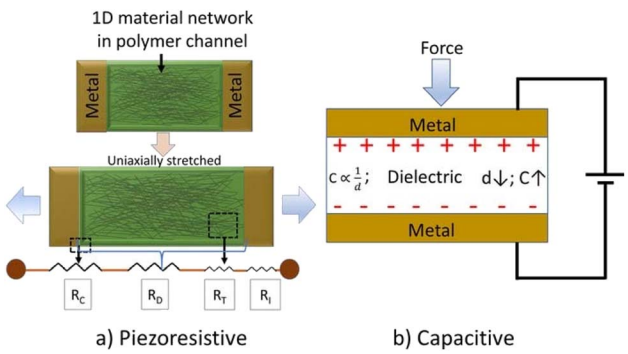

Fig. 2 Schematic diagram of the sensing mechanism of piezoresistive and capacitance-type flexible sensors[71] (Copyright 2020, The Electrochemical Society).

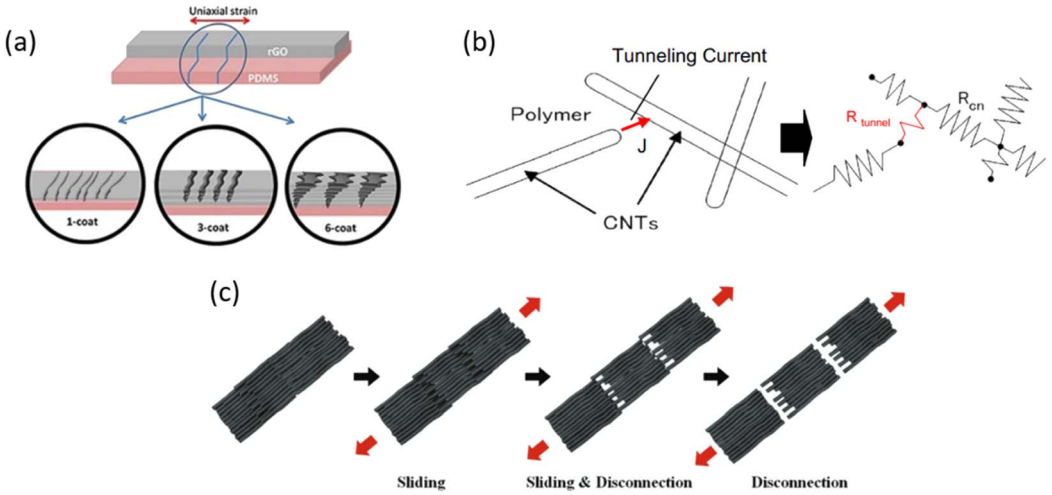

Fig. 3 Three sensing mechanisms: (a) crack propagation[72] (Copyright 2017, Macmillan Publishers Ltd); (b) tunneling effect[74] (Copyright 2008, Elsevier); (c) disconnection mechanism[76] (Copyright 2019, Wiley).

the increasing deformation will gradually lengthen the tunnel distance, resulting in the increase in the resistance. When the deformation recovers, the length of the tunnel will also recover and the resistance will gradually decrease.

The disconnection mechanism[76,77] means that the conductive fillers form a conductive path on the surface or inside of the flexible material, and the conductive fillers will be connected or overlapped with each other. When the flexible sensor generates strain, the overlap between the conductive fillers will gradually decrease until it is disconnected with the gradual increase in strain, resulting in the reduction of the conductive path and the increase in the resistance of the flexible sensor. With the gradual recovery of the strain, the disconnected conductive path will be connected again, thus reducing the resistance of the flexible sensor.

The current research shows that the above three mechanisms do not appear alone in the piezoresistive flexible sensor, usually one sensing mechanism is the main, and two or three mechanisms are combined with each other. In addition, the research on the sensing mechanism is not perfect at present. For example, there are often "shoulder peaks" in the testing process of flexible sensors. At present, it is considered that the emergence of "shoulder peaks" is related to the competition between the disconnection and reconnection of the conductive path, but the specific mechanism needs to be further studied (Fig. 3).

3 Common materials of piezoresistive flexible sensor

3.1 Flexible substrate material

The flexible substrate material of flexible sensor needs to meet the requirements of good flexibility, light weight, and excellent mechanical properties. This paper mainly introduces the research progress of flexible human electronic sensors based on PDMS and modified polysiloxane elastomer.

3.1.1 PDMS as flexible substrate. PDMS is a type of polysiloxane material that possesses many excellent physical and chemical properties. Therefore, it is widely used in the matrix materials of flexible sensors. Jin[78] *et al.* prepared a high elastic strain sensor with PDMS as the fibrous flexible matrix and MWCNT as the outer wall of the conductive material. The sensor has a wide detection range (1–100%), excellent sensitivity, and good mechanical properties. The material has a good application prospect in the field of flexible wearable sensors. Paul[79] *et al.* prepared a thin-film composite structure using vertically arranged carbon nanotubes (VACNT) and PDMS. The strain sensing range of the sensor is 0.004–30%. At 30% strain, the GF is as high as 6436.8, and its response time is as low as 12 ms. After 10 000 tensile cycles, it still retains its original performance. Song[80] *et al.* prepared a hollow-structured MXene PDMS composite. The material has a wide bending angle detection range from 0° to 180°, a long-term reliability of up to 1000 cycles, and a pressure detection limit as low as 10 mg, which can detect small actions such as swallowing and facial muscle movement.

3.1.2 Modified polysiloxane material as a flexible substrate. Although PDMS as a flexible substrate has many advantages, with the development of flexible electronic materials, it is found that PDMS as a flexible matrix alone will have some performance defects compared with modified polysiloxane materials. For example, compared with modified polysiloxane materials, PDMS has lower toughness and tear strength. More importantly, it is difficult for the flexible sensor to avoid damage such as scratches in real use. If the flexible material does not have self-repair performance, it will reduce the safety of the sensor and the accuracy of detection. Therefore, it is a research hotspot to endow flexible sensors with self-healing performance.

Shan[81] *et al.* prepared a new sensor based on self-healing silicone elastomer and polypyrrole (PPy). First, the amino-terminated polydimethylsiloxane and hexamethylene diisocyanate (HDI) were synthesized into a prepolymer, and then 2,6-

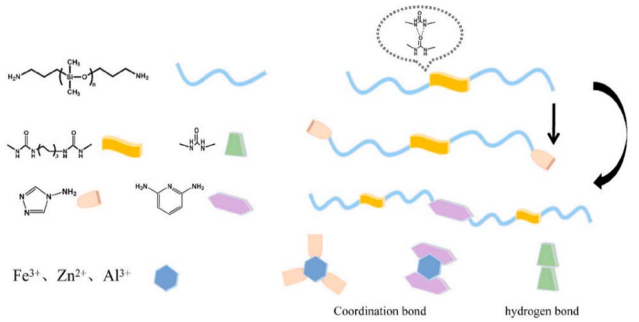

Fig. 4 Preparation flow chart of self-repairing silicone elastomer[81] (Copyright 2022, Elsevier).

diaminopyridine (DAP) was added for the chain extension reaction to introduce metal ions into the system to endow it with self-healing performance. Finally, PPy was attached to the surface of silicone elastomer by the original polymerization method. The preparation process is shown in Fig. 4. The prepared self-healing flexible sensor has a strength of 0.88 MPa and an elongation at break of 652.5% after healing. The sensor has a wide detection range of 130% and a GF of 1251. After cutting, the sensing performance can still be maintained with reliability and stability. The strain sensor developed has broad application prospects in intelligent flexible equipment, providing a valuable method for developing human motion monitoring sensors with excellent comprehensive performance.

Tang[82] *et al.* prepared an ultrafast self-healing polysiloxane self-adhesive electronic skin. The author's team synthesized a block copolymer of 1,4-dithiothreitol (DTT) and PDMS, and then added boric acid (BA) to form a dynamic borate ester matrix with a large number of hydroxyl groups in the chain. Finally, self-healing elastomer and silver nanowire (AgNW) film are compounded to prepare self-repairing flexible electronic skin. The synthesis path is shown in Fig. 5. The prepared new polysiloxane flexible electronic skin has a mechanical strength of up to 0.43 MPa and an elongation at break of 1500%. When the material is damaged, 100% of the original mechanical properties can be restored in 30 s at room temperature, and the sensing performance can be restored in only 1 s. It is the fastest self-healing flexible sensor to repair so far. This flexible sensor has broad application prospects in the health monitoring of underwater activities such as swimming and underwater rehabilitation exercises.

Zhang[83] *et al.* modified MXene and amino polydimethylsiloxane based on esterification and Schiff base reaction, respectively. The preparation process is shown in Fig. 6. The modified composite system contains a large number of hydrogen bonds and imine bonds, which endows the sensor with ideal tensile properties and efficient self-healing ability. The mechanical strength of the prepared flexible sensor reaches 1.81 MPa. When the material is damaged and repaired at room temperature for 24 h, the tensile properties and conductivity recover to 98.4% and 97.6%, respectively, and the sensor can detect small actions such as speaking and swallowing.

Zhang[84] *et al.* grafted thioctic acid (TA) onto polydimethylsiloxane containing amino group in the side chain and built a dynamic crosslinking network based on S–Au by introducing gold nanoparticles. As shown in Fig. 7, the material can heal rapidly under near-infrared radiation, with a repair efficiency of 92%, and the sensor has a very high detection range (up to 250% strain) and GF of 3.6. It can monitor human motion such as joint bending.

3.2 Conductive filler

The conductive fillers commonly used in flexible sensors can be divided into three categories: metal conductive materials, conductive polymer materials, and carbon conductive materials.

3.2.1 Metal conductive materials. Metal conductive materials mainly include metal nanowires and metal nanoparticles. At present, metal nanoparticles mainly include silver nanoparticles and gold nanoparticles. Metal nanowires include copper nanowires, gold nanowires, and silver nanowires. Considering the cost and conductivity of materials, silver nanowires are the most commonly used. Yin[85] *et al.* prepared silver nanowire film by water bath spinning method and embedded it into PDMS to prepare the PDMS/AgNWs flexible

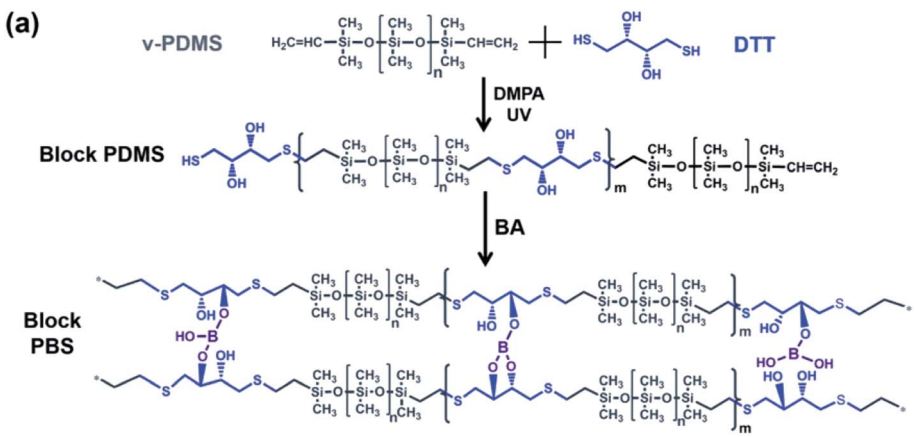

Fig. 5 Synthetic path of polysiloxane self-healing elastomer[82] (Copyright 2022, Royal Society of Chemistry).

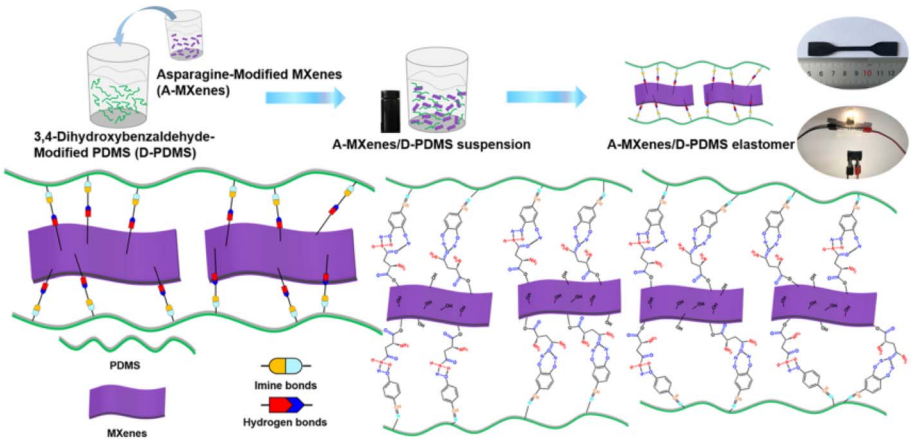

Fig. 6 Preparation flow chart of the MXene/PDMS self-repairing flexible sensor[83] (Copyright 2020, The American Chemical Society).

strain sensor. The sensor has extremely excellent transparency. The light transmittance at 550 nm wavelength reaches 86.3%, and the sensitivity is excellent. The GF can reach 86.4. The sensor has reliable response to human motion signals. Kong[86] *et al.* creatively prepared a highly scalable AgNWs/PDMS fiber strain sensor with a spiral structure. The preparation process is shown in Fig. 8. The unique spiral structure enables the sensor to have a wide sensing range of 100% strain, excellent linearity, negligible hysteresis and up to 3.0 GF. The sensor can not only detect the joint bending when the human body is moving but also control the brightness of the bulb connected to the sensor according to the joint bending degree.

3.2.2 Polymer conductive materials. At present, common conductive polymers mainly include polypyrrole (PPy),

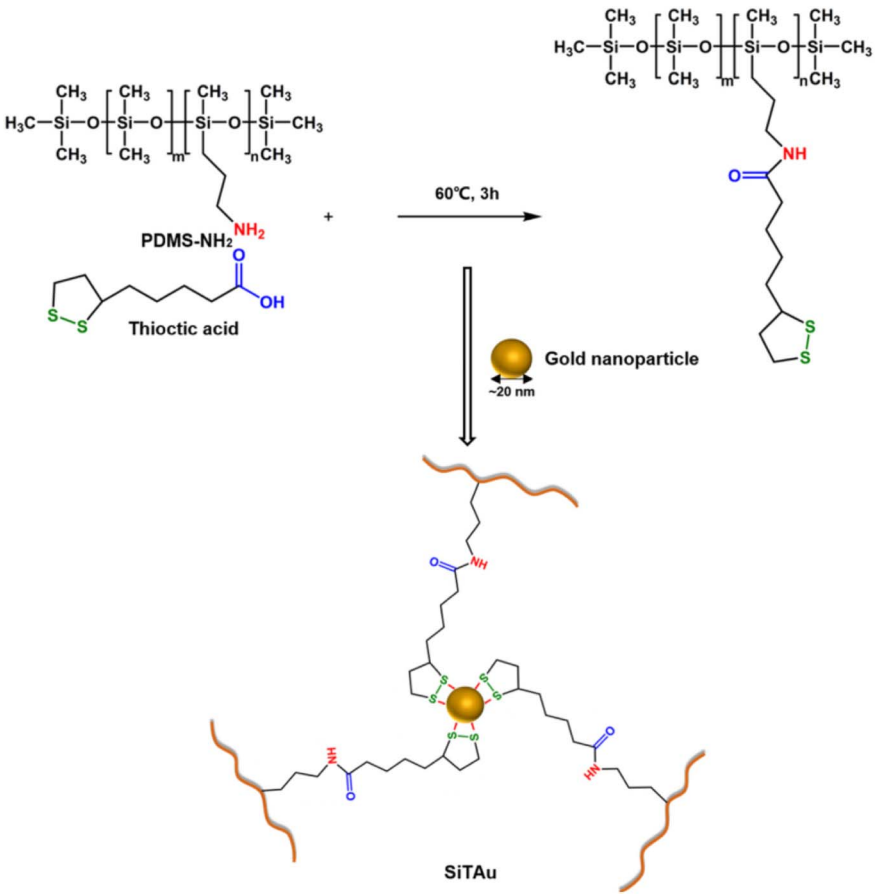

Fig. 7 Preparation mechanism of AuNP/PDMS self-repairing flexible sensor[84] (Copyright 2021, Elsevier).

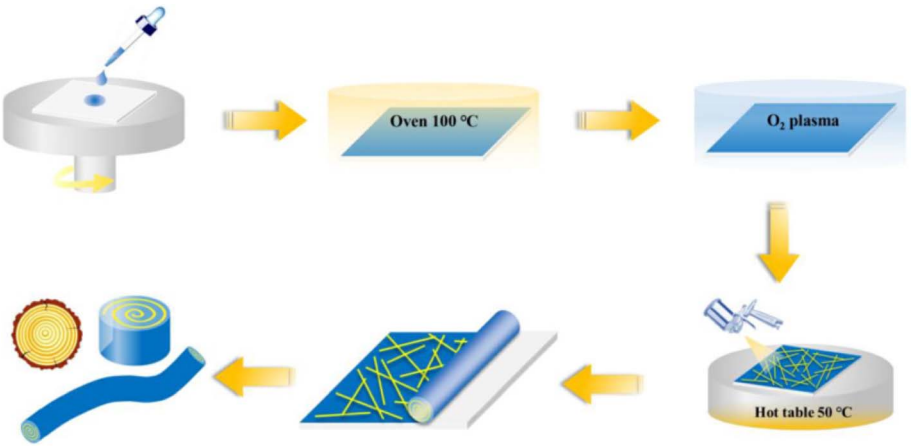

Fig. 8 Preparation process of the spiral structure AgNW/PDMS strain sensor[86] (Copyright 2021, Elsevier).

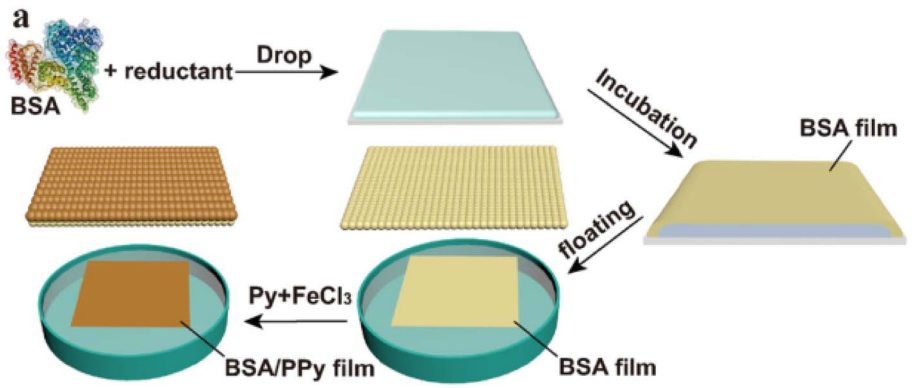

Fig. 9 Preparation flow chart of the BSA/PPy conductive film[88] (Copyright 2021, Elsevier).

polythiophene (PTh), and polyaniline (PANI).[87] PPy and PANI are commonly used in piezoresistive flexible sensors. Wang[88] *et al.* prepared a bovine serum albumin/polypyrrole (BSA/PPy) mixed film and compounded the mixed film with PDMS film to prepare a self-adhesive flexible sensor. The preparation process is shown in Fig. 9. The sensor can withstand more than 500 bending cycles and can dynamically adjust the conductivity of PPy according to external strain.

Zheng[89] *et al.* designed a flexible wearable pressure sensor with hollow structure and micro convex surface structure based on polyaniline/polydimethylsiloxane (PANI/PDMS) composites. The preparation process is shown in Fig. 10. Due to the existence of hollow structure and micro convex surface structure, the sensitivity and linearity of the sensor are greatly improved. The sensitivity of the sensor is 0.641 kPa^{-1} in the range of 0.05–60 kPa, which can stably cycle for more than 6000 times, and the response time and recovery time are as low as 200 ms and 150 ms respectively.

Jiang[90] *et al.* prepared the nanofiber film based on AgNWs/PANI/PU and then encapsulated the nanofiber film with PDMS to prepare a wearable strain sensor. The preparation process is shown in Fig. 11. The sensor has excellent antifouling performance and linearity. The synergy of PANI and AgNWs endows the sensor with high sensitivity. In the range of 0–35% strain, the GF reaches 59, and the sensor has reliable anti-fatigue performance and signal stability. It has broad

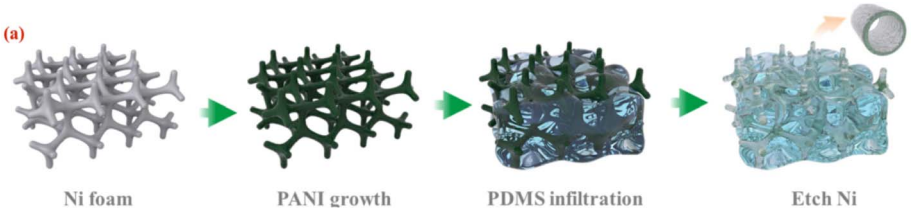

Fig. 10 Preparation flow chart of the PANI/PDMS pressure sensor[89] (Copyright 2021, Elsevier).

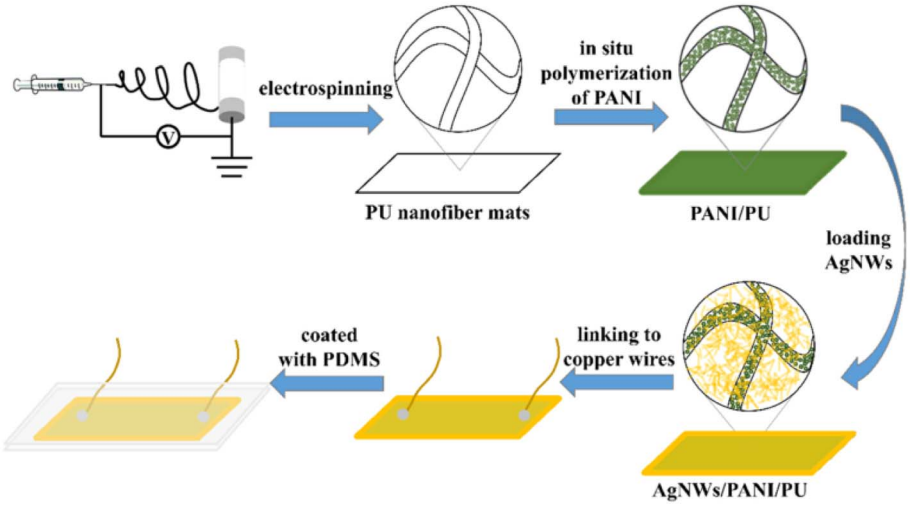

Fig. 11 Preparation flow chart of the AgNWs/PANI/PU strain sensor encapsulated by PDMS[90] (Copyright 2021, Elsevier).

application prospects in human health management, sports monitoring, and other fields.

3.2.3 Carbon-based conductive materials. At present, in the field of piezoresistive flexible sensors, carbon-based materials are the most commonly used conductive fillers, including carbon nanotubes (CNT), graphene (GR), carbon black (CB), and MXene.

A Carbon nanotubes. Carbon nanotubes (CNTs) are one-dimensional nanomaterials with excellent mechanical properties, electrical conductivity, and low percolation threshold.[91] Single-walled carbon nanotubes are difficult to prepare, resulting in high cost. Therefore, multiwalled carbon nanotubes are widely used in the field of flexible sensors.[92] Zhu[93] *et al.* used PDMS as a flexible matrix and carbon nanotube (CNT)-cellulose silylated nanocrystalline (SCNC) as a conductive filler to prepare a high-performance flexible sensor. The preparation process is shown in Fig. 12. The sensor has a tensile strength of up to 5.75 MPa, a strain sensing range of up to 100%, and a GF of 37.11 at 50–100% strain. The sensor has long-term stability and durability and has broad application prospects in the field of wearable electronic devices.

Wang[94] *et al.* prepared a three-layer CNT/PDMS flexible sensor. The preparation process is shown in Fig. 13. The sensor has a wide strain measurement range of more than 50%, GF can reach 207, response time is less than 10 ms, and the sensor still has excellent stability after up to 10 000 load cycles.

Inspired by cephalopods, Zhang[95] *et al.* prepared a self-healing MWCNT/PDMS flexible sensor. By introducing

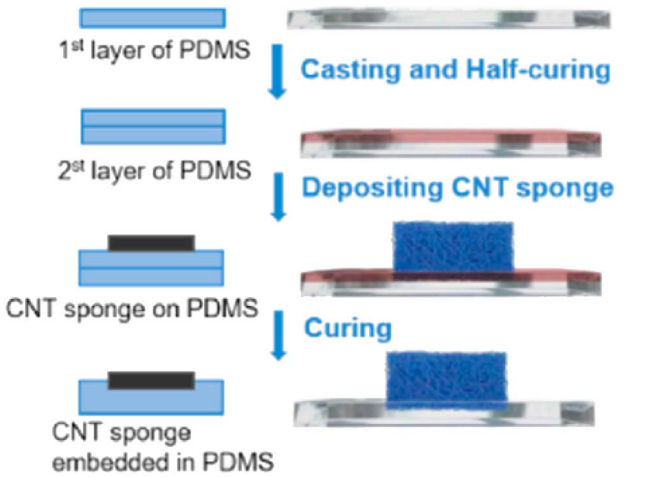

Fig. 13 Preparation process of three-layer PDMS/CNT flexible sensor[94] (Copyright 2021, Elsevier).

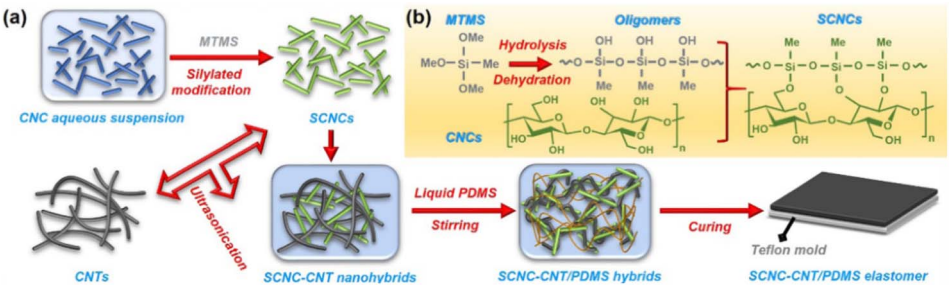

Fig. 12 (a) SCNC-CNT/PDMS flexible sensor preparation process. (b) SCNC synthesis path diagram[93] (Copyright 2021, The American Chemical Society).

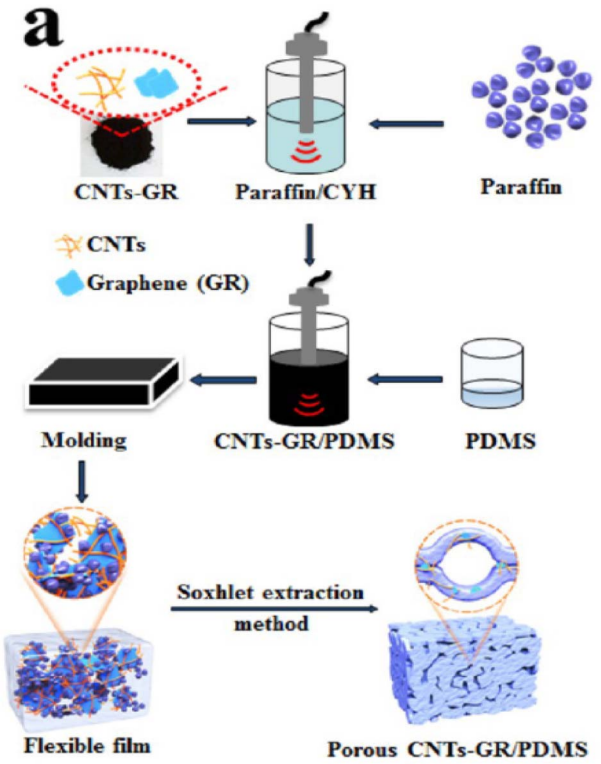

Fig. 14 CNTs-GR/PDMS flexible sensor preparation process[97] (Copyright 2021, The American Chemical Society).

carboxyl groups into carbon nanotubes and silicone main chains and then adding metal ions to form metal coordination bonds, the material was endowed with self-healing performance. The GF value of the synthesized self-healing flexible sensor was 3.8673, with a tensile strength of up to 1.77 MPa and a maximum strain of 348%. The repair efficiency of the sensor at room temperature is as high as 91%, which can meet the needs of motion monitoring and other fields.

B Graphene. Graphene (GR) is a two-dimensional cellular carbon material, which has excellent specific surface area, mechanical properties, electrical conductivity, and stability,[96] making it a good candidate for flexible sensors. He[97] *et al.* used Soxhlet extraction technology to prepare a CNTs-GR/PDMS flexible sensor with microporous structure. The preparation process is shown in Fig. 14. The sensor has excellent sensitivity. In the strain range of 0–3%, 3–57%, 57–90%, and 90–120%, the GF reaches 182.5, 45.6, 70.2, and 186.5, respectively, and the sensor also has a very low detection limit (0.5% strain) with fast response time (60 ms) and durability of up to 10 000 load cycles. The sensor has broad application prospects in the field of wearable electronic devices.

Niu[98] *et al.* prepared a GR/AgNWs composite conductive material and encapsulated it with PDMS to prepare a flexible strain sensor that can work at very low temperature (−40 °C). The sensor has excellent fatigue resistance, very low hysteresis, and near zero temperature resistance coefficient (TCR). Under the condition of more than 36% strain, the GF is as high as 9156. The sensor can monitor various human actions at room temperature and low temperature. Iqra[99] *et al.* prepared a reduced graphene oxide (RGO)/PDMS flexible sensor by laser marking. The sensor has high sensitivity. When the strain range is 0–140%, 0–130%, and 0–11.1%, the GF reaches 12.1, 3.5, and 90.3, respectively. The sensor can monitor joint and muscle movement and has a broad application prospect.

C Carbon black. Carbon black (CB) is an amorphous zero-dimensional carbon material with good conductivity.[100,101] Carbon black can be divided into different types according to the particle size. The flexible sensor made of carbon black with small particle size has high conductivity due to the large

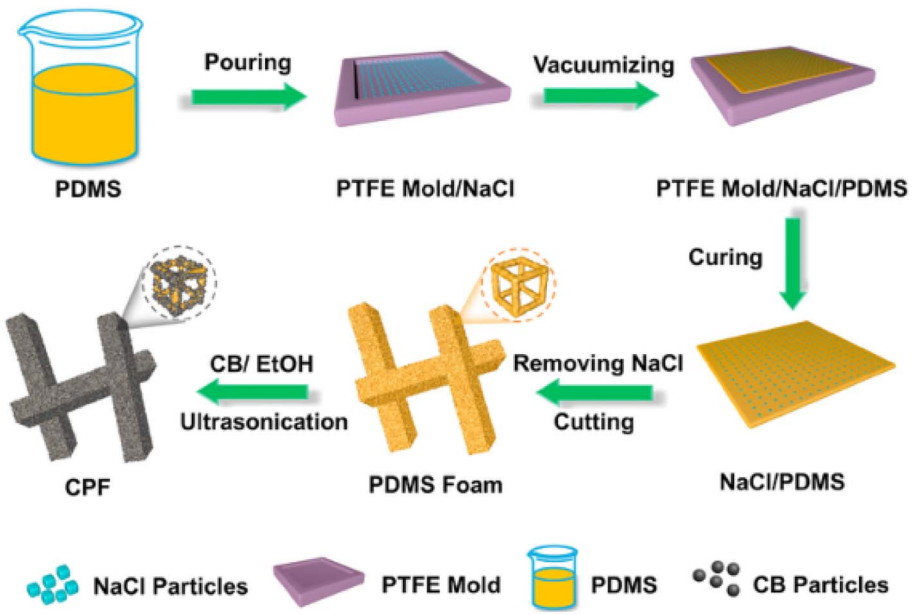

Fig. 15 CB/PDMS conductive foam material preparation process[105] (Copyright 2021, Elsevier).

number of conductive particles per unit volume, but carbon black with small particle size will agglomerate, affecting the mechanical properties of the sensor.[102] The current research shows that the flexible sensor prepared with carbon black as the conductive filler has poor stability because the conductive path formed by carbon black will be destroyed and reconstructed when the flexible sensor is deformed.[103] Therefore, in recent years, researchers are committed to preparing high stability flexible sensors with carbon black as the conductive filler. Li[104] *et al.* used nanocarbon black (CB) and carbon nanotubes (CNTs) as mixed conductive fillers and modified by PDMS to prepare a flexible strain sensor. The sensor has excellent mechanical properties and superhydrophobicity with an elongation at break of 996.5%, GF of 648.83 in the strain range of 979.9–996.5%, and its performance is still stable after 1000 load cycles of 100% strain. Xia[105] *et al.* prepared a CB/PDMS foam material for strain sensing. The preparation process is shown in Fig. 15. The material has a solid three-dimensional conductive network, good linearity, and wide strain sensing range (70% strain). Due to the strong interaction between conductive filler and PDMS, the material has very low hysteresis (less than 1.2%). With fast response time (100 ms) and durability of more than 20 000 load cycles, the material shows great application potential in the field of flexible sensors.

Hu[106] *et al.* designed and prepared a strain sensor based on double-layer hybrid structure, which is composed of carbon black conductive layer and PDMS flexible layer. The sensor has high sensitivity and up to 100% strain sensing range. In addition, the sensor also has good durability and can withstand more than 10 000 load cycles of 60% strain.

D MXene. MXene material was first prepared by researchers at Drexel University in 2011 by selectively etching the Al layer in the ternary layered carbide Ti_3AlC_2 with hydrofluoric acid.[107] MXene is a kind of two-dimensional layered material with a graphene-like structure composed of transition metal carbides or nitrides. MXene has the characteristics of typical two-dimensional layered structure, such as large specific surface area and excellent conductivity,[108] and MXene has rich surface groups,[109] which is convenient for modification. Therefore, MXene material has a broad application prospect in the field of flexible electronic sensors. Luo[110] *et al.* constructed a waterproof and breathable smart textile with multicore-shell structure by decorating MXene on polydopamine (PDA)-modified elastic fabric and coating it with PDMS. The material has a large temperature working range (25–100 °C) and excellent temperature resistance coefficient (−1.8%/°C). In addition, the smart textile has high sensitivity. Under the working strain of 0–45%, the GF reaches 18, and the material has good recycling and durability. Zhang[111] *et al.* used thermoplastic polyurethane (TPU) as the base material to prepare highly conductive and stretchable Ti_3C_2 MXene/TPU sensing elements by the simple spraying process and encapsulated the sensing elements in PDMS to obtain a MXene TPU/PDMS flexible strain sensor with excellent performance. The preparation process is shown in Fig. 16. The strain sensor has a low detection limit (less than 0.005%, 0.5 μm), wide sensing range (0–90%), short response time (120.1 ms), good durability (>3000 cycles), *etc.*

Xu[112] *et al.* combined carbon nanotube (CNT) and MXene onto porous PDMS sponge and developed a multifunctional strain sensor. The preparation process is shown in Fig. 17. The sensor has wide sensing range (105% strain), high sensitivity (GF = 1939), fast response (158 ms), and sufficient reliability under repeated stretching, compression, and bending cycles. The sensor has broad application prospects in human motion monitoring, medical health, and other fields.

To sum up, according to the current research, the above three types of conductive fillers are used in resistance flexible sensors, of which carbon-based conductive fillers are the most widely used. At present, carbon-based conductive fillers can be divided into four types: carbon nanotube (CNT), carbon black (CB), graphene, and MXene. The four types of conductive fillers have their own advantages and disadvantages when used alone, for example, when CNT is used as the conductive filler alone, the GF is relatively low, and its durability is poor. When graphene or MXene is used alone, the sensor's stretchability is too low. Therefore, researchers use two or more kinds of conductive fillers to pursue more balanced sensor performance. Chen[113]

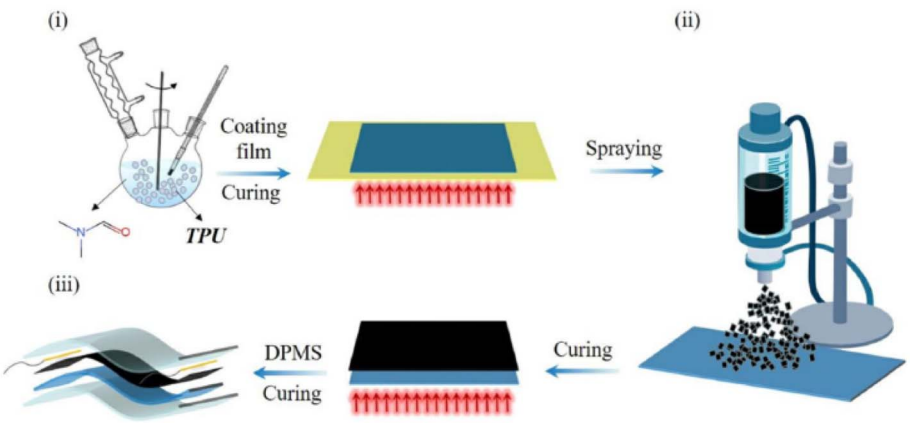

Fig. 16 Preparation flow chart of the MXene TPU/PDMS flexible strain sensor[111] (Copyright 2021, Elsevier).

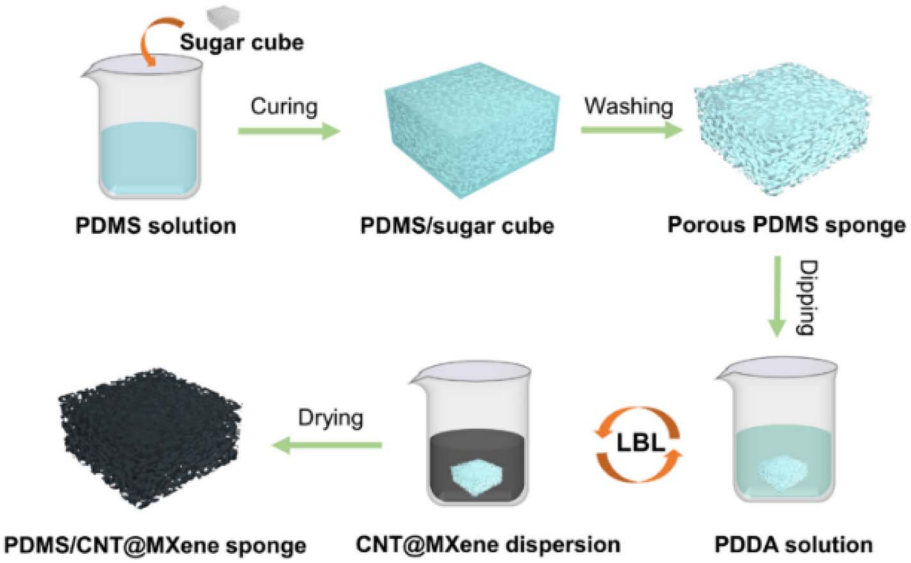

Fig. 17 Spongy PDMS/CNT@MXene flexible sensor preparation process[112] (Copyright 2022, Elsevier).

et al. prepared a PDMS/rGO/MWCNT porous aerogel flexible sensor. The composite conductive layer of graphene and carbon nanotubes endows the sensor with excellent stability. The GF of the sensor is as high as 18.55. After 900 times of reciprocating stretching under 20% strain, the sensor still has stable sensing performance. The sensor has a remarkable effect in monitoring the opening and closing of packaging and human movement, which provides a new idea for applying intelligent packaging and developing wearable electronic devices.

4 Preparation process of piezoresistive flexible sensor

To improve the performance of the flexible sensor, researchers have developed a variety of preparation processes to endow the sensor with various new structures. At present, there are mainly the following processes for the combination of the flexible substrate and the conductive filler in the piezoresistive flexible sensor, which are sandwich type, embedded type, filled type, and adsorption type.

4.1 Sandwich type

The fabrication process of the flexible sensor with the sandwich structure is to clamp the conductive filler between two layers of flexible matrix materials. Generally, one layer of flexible substrate is coated with conductive filler, and then another layer of flexible substrate is used to package the conductive filler. Jiang[114] *et al.* prepared a sandwich structure self-healing flexible sensor based on silver nanowires and polydimethylsiloxane and enhanced the sensor with carbon fiber (CFS). The sensor has a large sensing range (0–60%), high sensitivity (GF = 1.5), excellent tensile strength (10.3 MPa), and excellent reliability. Chen[115] *et al.* prepared a sandwich-shaped PDMS/CNTs/PDMS flexible sensor. The preparation process is shown in Fig. 18. The sensor has good light transmittance, extremely wide strain sensing range (0–130%), and can recognize small actions such as facial expressions.

Liu[116] *et al.* coated reduced graphene oxide (RGO) on the surface of polystyrene (PS) microspheres, mixed with silver nanowires (AgNWs) to prepare conductive fillers, and sandwiched them between two layers of PDMS to prepare sandwich

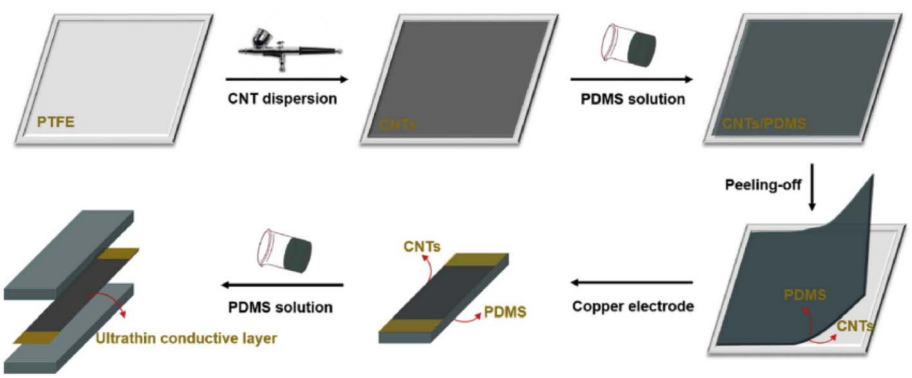

Fig. 18 Preparation flow chart of sandwich PDMS/CNTs/PDMS flexible sensor[115] (Copyright 2020, Elsevier).

PDMS/PS@RGO/AgNWs/PDMS flexible sensor, which has excellent strain working range (0–230%), high sensitivity (GF = 47), detection limit as low as 1% strain, and excellent reliability and linearity.

4.2 Embedded type

The preparation process of embedded flexible sensor is to embed conductive filler into the surface of flexible substrate. The common preparation method is to prepare the conductive layer first and then package it with uncured flexible substrate. Embedded flexible sensors have been widely researched by researchers because of their high stability. Xu[117] *et al.* used carbon nanotube (CNT) and $Ti_3C_2T_x$ MXene to blend and prepare the conductive composite film and then embedded the composite film into the PDMS matrix to prepare an ultrastable and cleanable embedded flexible sensor. The preparation process is shown in Fig. 19. The sensor has excellent anti-interference ability, and the resistance change is less than 10% within the temperature range of −20–80 °C or after 120 min of ultrasound in water. In addition, the sensor has high sensitivity, GF up to 13.3, and has broad application prospects in the field of human-motion monitoring.

4.3 Filled type

The preparation process of the filled flexible sensor is to disperse the conductive filler in the uncured flexible matrix by stirring and then cure to prepare the filled flexible sensor.[102] However, to make the conductivity of the filled flexible sensor meet the requirements, it is usually necessary to add a large number of conductive fillers into the flexible substrate, and a large number of conductive fillers will reduce the flexibility of the flexible substrate and increase the percolation threshold. Therefore, how to solve these problems is the focus of researchers. Chen[118] *et al.* added silica particles into flexible PDMS/MWCNT composites (μSiO_2), a filled flexible sensor is prepared, and its preparation process is shown in Fig. 20. The results show that the addition of silica particles effectively reduces the percolation threshold and improves the sensitivity (GF = 62.9).

Du Jian[119] mixed carbon nanotube (CNT) and PDMS to prepare a filled CNT-PDMS flexible sensor. The research shows that 8 wt% CNT-PDMS composite has a 40% strain sensing range and high sensitivity (GF = 1.2097). The material can capture the mechanical signal of finger joint bending and can be applied to the heel of the sole to monitor the frequency of walking or running.

Zheng[121] *et al.* used a simple solution mixing method to prepare a strain sensor based on the blending of PDMS with carbon nanotubes (CNT) and carbon black (CB). Due to the bridging effect of carbon nanotubes on carbon black, the sensor has a strain sensing range of up to 300% and excellent durability (it can withstand 2500 cycles under 200% strain). Also, the sensor has good sensitivity (GF up to 13.3), which has a broad application prospect in the field of human motion monitoring.

4.4 Adsorption type

The preparation process of the adsorption type flexible sensor involves the immersion of the flexible substrate into the suspension prepared by the conductive filler so that the conductive filler can be adsorbed on the surface of the flexible substrate to form a conductive network. As mentioned above, Luo[110] *et al.* constructed an adsorption type flexible sensor with multicore-shell structure by immersing polydopamine (PDA)-modified elastic fabric in the MXene suspension and coating it with PDMS. Its structure is shown in Fig. 21. The material has a large temperature operating range (25–100 °C) and excellent temperature resistance coefficient (−1.8%/°C). In addition, the smart textile has high sensitivity. Under a working strain of 0–45%, the GF reaches 18, and the material has good recycling and durability.

To sum up, at present, the piezoresistive flexible sensor has the above four common preparation processes, and its

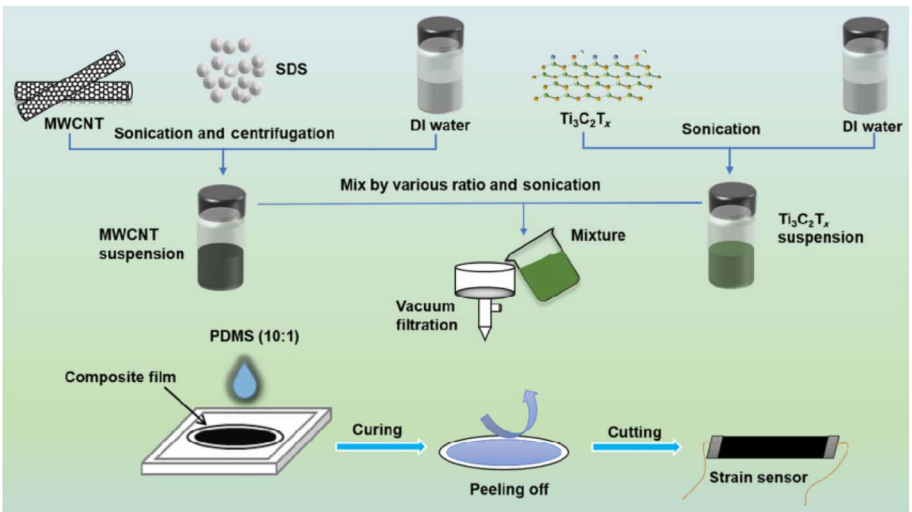

Fig. 19 Preparation process of embedded CNT MXene/PDMS flexible sensor[117] (Copyright 2021, Springer).

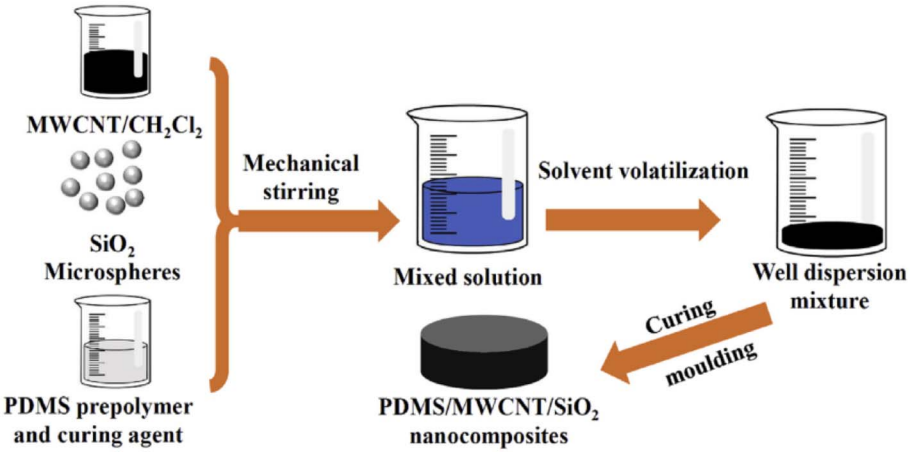

Fig. 20 Preparation process of the filled PDMS/MWCNT/SiO_2 flexible sensor[118] (Copyright 2019, Elsevier).

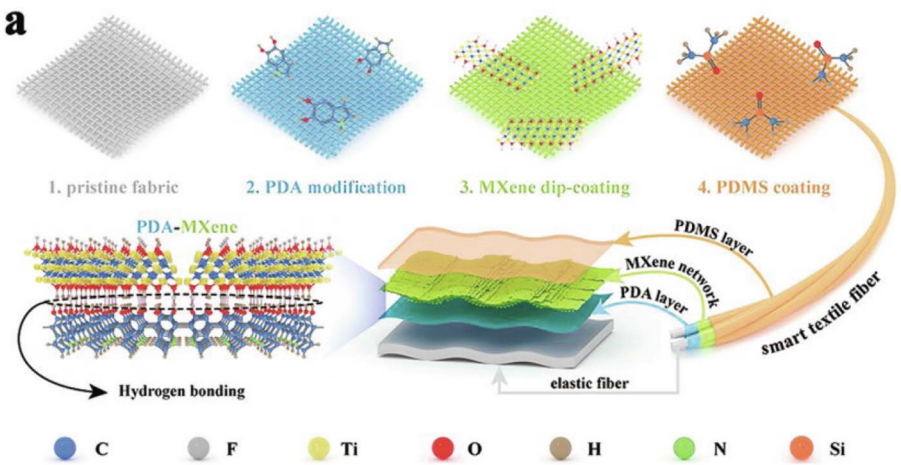

Fig. 21 Structural diagram of the adsorption PDA MXene/PDMS flexible sensor[110] (Copyright 2021, Elsevier).

performance has its own advantages and disadvantages. For example, sandwich sensors generally have the sensitivity that can meet the use requirements, but the preparation cost is high and the durability is poor. The sensitivity, sensing range, linearity, and other properties of the filled sensor needs to be improved, but its preparation cost is low, which is suitable for mass production in the industry. The preparation of the adsorption sensor is complex, and according to the different structure and performance of the sensor, the embedded sensor has high durability and linearity and is stable in daily use. It is one of the main research directions at present. How to improve the sensitivity and preparation cost of the embedded sensor needs further research. Fig. 22 summarizes the sensitivity and sensing range of the sensor using various preparation processes to facilitate the reader to visually compare the performance of the sensor.

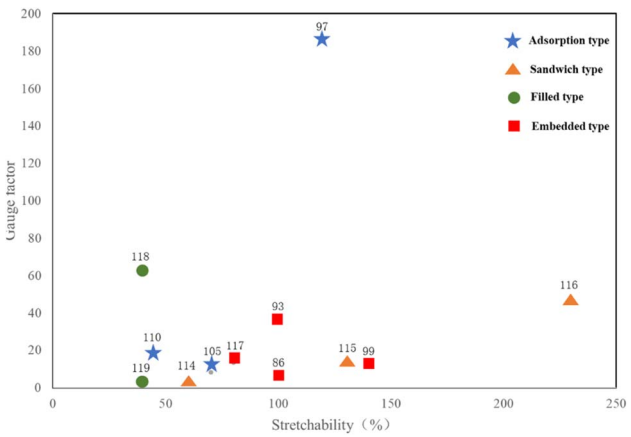

Fig. 22 Performance comparison of some polysiloxane piezoresistive flexible sensors prepared by different processes.

5 Performance parameters of piezoresistive flexible sensor

The piezoresistive flexible sensor can transform the mechanical signals of human motion into electrical signals to realize the monitoring of human motion and health. The performance of

the resistive flexible sensor can be evaluated by different parameters, including strain sensing range, gauge factor (GF), durability, and linearity. Each of these parameters is very important to the performance of the resistive flexible sensor.[133,134]

5.1 Strain sensing range

The strain sensing range represents the ability of the sensor to withstand a certain tensile length without permanent deformation and still maintain the sensing performance. The piezoresistive flexible sensor based on polysiloxane usually shows different strain sensing ranges according to its conductive filler and preparation process. Flexible sensors prepared with MXene or graphene as conductive filler alone usually show a low strain sensing range (less than 20%), and the strain sensing range of flexible sensors prepared with silver nanowires, carbon black, and polymer conductive materials is significantly improved, which can reach about 100%. However, the flexibility prepared with carbon nanotubes usually shows the highest strain sensing range (higher than 200%).

Not only the selection of conductive fillers but also the different preparation processes of the sensor will affect the strain sensing range of the sensor. Current research shows that the comprehensive performance of filled type flexible sensors is poor, with a strain sensing range typically below 60%.[118,119] The other three types of flexible sensors have similar strain sensing range, typically reaching over 100%.[101–117]

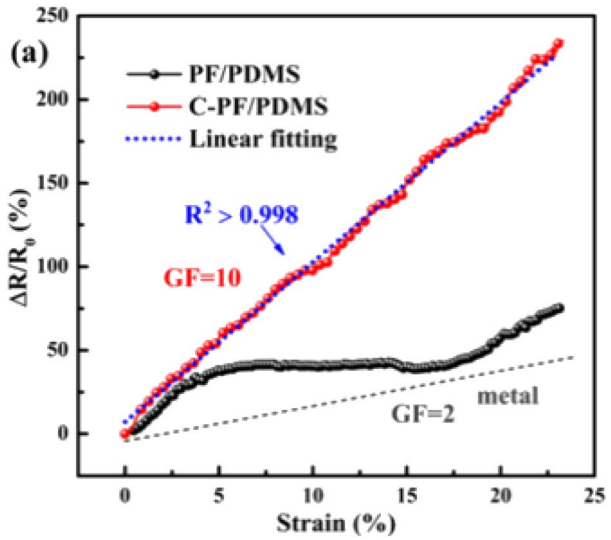

Fig. 23 Relative resistance change strain curve[121] (Copyright 2019, Elsevier).

5.2 Gauge factor (GF)

The value of gauge factor (GF) is the ratio of relative resistance change to strain,[120] which is used to characterize the relative resistance change strain curve of GF. As shown in Fig. 23, the value of GF can directly reflect the sensitivity of the sensor. The higher the value of GF, the higher the sensitivity of the sensor, and the better the performance. The calculation method is shown in formula (1)

$$\mathrm{GF} = \frac{\Delta R - R_{\mathrm{O}}}{\varepsilon} \quad (1)$$

where, ΔR represents the change of resistance after strain is applied, R_{O} represents the initial resistance, and ε refers to the strain applied to the sensor.

GF is mainly affected by the type, amount, and preparation process of conductive fillers. The current research shows that if only one conductive filler is used, polypyrrole (PPy) has excellent sensitivity (GF greater than 1000), followed by MXene with high sensitivity (GF greater than 400). However, when MXene is used alone the conductive filler, there will be a problem of poor sensor extensibility. Compared with the single conductive filler, the suitable GF can be obtained by mixing two different conductive fillers, and the comprehensive performance of the sensor can also be improved. As mentioned above, Xu[112] *et al.* combined carbon nanotubes (CNT) and MXene to porous a PDMS sponge and developed a strain sensor with porous

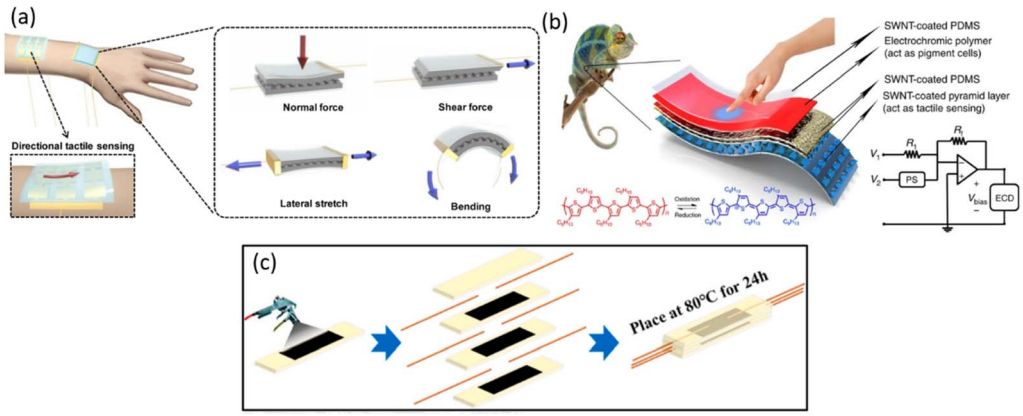

Fig. 24 (a) Structural diagram of the PDMS/CNT flexible sensor[122] (Copyright 2014, The American Chemical Society); (b) structural diagram of PDMS/SWNTs flexible sensor[123] (Copyright 2015, Nature); (c) structural diagram of layered PDMS/CNTs flexible sensor[125] (Copyright 2021, Elsevier).

structure. The sensor has high sensitivity (GF up to 1939) and excellent strain sensing range (105% strain) in repeated stretching sufficient reliability under compression and bending cycles. To sum up, if it is necessary to improve the sensitivity of the sensor, it is a reliable method to mix a variety of conductive fillers and give the sensor a new structure.

In addition, GF can also be improved by changing the sensor structure, for example, biomimicry,[122–124] porous,[97,105,112] and layered.[106,125] Biomimetic structures often have different sensitivities due to different structural designs. Park[122] *et al.*, inspired by the interlocking microstructure in human skin, prepared a filled type PDMS/CNT flexible sensor with a piezoresistive interlocking microsphere array structure. The structure is shown in Fig. 24(a). Due to its unique structural design, the sensor has excellent sensitivity (GF up to 1084). In addition, the sensor also has a strain sensing range of up to 120%, which can respond quickly to small strains within 18 ms. This material can be applied in robot skin, prosthetics, and rehabilitation equipment to monitor the movement and pressure distribution. Chou[123] *et al.* were inspired by the pyramid shaped microstructure on the skin of a chameleon to prepare a PDMS/SWNTs stretchable electronic skin (e-skin), as shown in Fig. 24(b). The material can easily control the color of the e-skin by changing the applied pressure and the duration of the applied pressure. Due to its unique pyramid shaped microstructure design, the sensitivity of the e-skin is moderate (GF = 3.3) but it has excellent linearity. This material is expected to be applied to interactive wearable devices, artificial prosthetics, and intelligent robots.

The layered structure shows a small increase in the sensitivity of the sensor, but it often endows the sensor with stability and high linearity. Zhou[125] *et al.* prepared a sandwich-layered PDMS/CNTs flexible sensor, as shown in Fig. 24(c). The sensor has high sensitivity (GF = 6.2) and cyclic stability at 90% strain. This material has broad application prospects in wearable devices and flexible sensors.

Porous structures can greatly enhance the sensitivity of sensors, but due to the large number of pores in their structure, their mechanical performance is often poor. As mentioned earlier, Xu[112] *et al.* prepared a porous PDMS/CNT@MXene Sponge, which has extremely high sensitivity (GF = 1939), a wide sensing range (105% strain), and a fast response speed (158 ms). However, its mechanical properties are poor, with a tensile strength of only 0.058 MPa. This sensor has potential application value in intelligent clothing, flexible electronics, and human health monitoring. He[97] *et al.* prepared a filled porous PDMS/CNT-GR flexible sensor. The sensor has excellent sensitivity (GF = 186.5), ultralow detection limit (0.5% strain), fast response time (60 ms), and excellent durability (10 000 cycles). The sensor can monitor various human movements; thus, it has broad application prospects in the field of intelligent wearable devices.

5.3 Linearity

Linearity is one of the key indicators for evaluating flexible sensors, which is defined as the percentage of the maximum deviation between the standard curve and the fitting line of the output signal.[126] The output signal of the sensor with high linearity is relatively accurate, and the post-processing of the output signal is simpler. The output signal of the sensor with low linearity is unstable and has large deviation, which makes the calibration process more difficult and the signal distorted. The current research found that the flexible sensor with a sandwich structure usually shows relatively high sensitivity, but its linearity is poor.[114–116] The embedded flexible sensor has the best linearity and stability.[86,98,117] The filled type sensor usually has the phenomenon of conductive filler agglomeration, resulting in poor linearity.[118,119,121] The adsorption flexible sensor has different linearity based on different structures of the sensor.[105,110,112] In addition, from the point of view of conductive fillers, the mixed use of a variety of conductive fillers is usually helpful to improve the linearity. As mentioned above, Xu[117] *et al.* blended carbon nanotubes (CNTs) and Ti_3C_2 MXene to prepare conductive composite films, and then embedded the composite films into the PDMS matrix to prepare an ultrastable

Table 1 Performance parameters of some polysiloxane resistance flexible sensors

		Performance parameter			
Material	Preparation process	GF	Sensing range	Linearity	References
AgNW/PDMS	Embedded type	3.0	100%	Linear	86
Ppy/PDMS-HDI-DAP	Adsorption type	1251	130%	Partial linearity	81
CNT-SCNC/PDMS	Embedded type	37.11	100%	Linear	93
Porous CNT/PDMS	Embedded type	207	50%	Partial linearity	94
Porous CNT-GR/PDMS	Adsorption type	186.5	120%	Partial linearity	97
RGO/PDMS	Embedded type	12.1	140%	Linear	99
CB/PDMS	Adsorption type	8.3	70%	Linear	105
PDA MXene/PDMS	Adsorption type	18	45%	Partial linearity	110
Porous CNT MXene/PDMS	Adsorption type	1939	105%	Partial linearity	112
CNTs/PDMS	Sandwich type	12.5	130%	Partial linearity	115
RGO AgNWs/PDMS	Sandwich type	47	230%	Partial linearity	116
CNT MXene/PDMS	Embedded type	13.3	80%	Partial linearity	117
CNT-SiO_2/PDMS	Filling type	62.9	40%	Nonlinearity	118
CNT/PDMS	Filling type	1.2	40%	Nonlinearity	119

and cleanable embedded flexible sensor. Compared with using Mxene alone or using carbon nanotubes alone as the conductive filler, the linearity of the sensor has been significantly improved. However, at present, the mechanism behind the linearity of the piezoresistive flexible sensor has not been fully studied. To improve the linearity of the sensor, in-depth theoretical research is needed.

5.4 Durability

The piezoresistive flexible sensor will inevitably produce a large number of load–unload cycles in actual use. If the durability of the sensor is poor, it can withstand relatively few load unload cycles, which will seriously affect the service life of the sensor. Current research shows that there are two main reasons for sensor failure, namely, permanent deformation of flexible substrate and fracture or sliding of the conductive layer.[127] Therefore, improving the mechanical properties of the flexible substrate and making the flexible substrate more firmly combined with the conductive filler are reliable methods to give the sensor durability. At present, a large number of researchers are committed to improving the durability of the sensor. For example, Hu[106] *et al.* designed and prepared a strain sensor based on a double-layer hybrid structure, which is composed of a carbon black conductive layer and a PDMS flexible layer. The sensor has good durability and can withstand more than 10 000 load cycles of 60% strain. Xia[105] *et al.* prepared a CB/PDMS foam material for strain sensing, which has a solid three-dimensional conductive network and can withstand the durability of 20 000 load cycles. Although the above research has greatly improved the durability of the flexible sensor, it will further improve the durability of the sensor if it can be endowed with self-healing. Therefore, the design of high-performance flexible sensor with self-healing capability is one of the current research hotspots.

In general, the above four performance parameters have an important impact on the performance of the sensor. Table 1 summarizes some performance indicators of the piezoresistive flexible sensor with polysiloxane as the flexible matrix so that the reader can more intuitively compare the performance of different flexible sensors.

6 Application prospect of the polysiloxane piezoresistive flexible sensor

Piezoresistive flexible sensors made of polysiloxane materials can be divided into piezoresistive pressure sensors and piezoresistive strain sensors, which are attached to the human skin to monitor human movement, pulse, heartbeat, and expression. Therefore, polysiloxane piezoresistive flexible sensors have broad application prospects, mainly reflected in the following two aspects.

6.1 Movement monitoring

Motion monitoring is one of the main application fields of piezoresistive flexible sensors. Motion detection can be divided into two types. One is to monitor the large-scale movement of bending joints such as elbows, knees, and fingers. In addition,

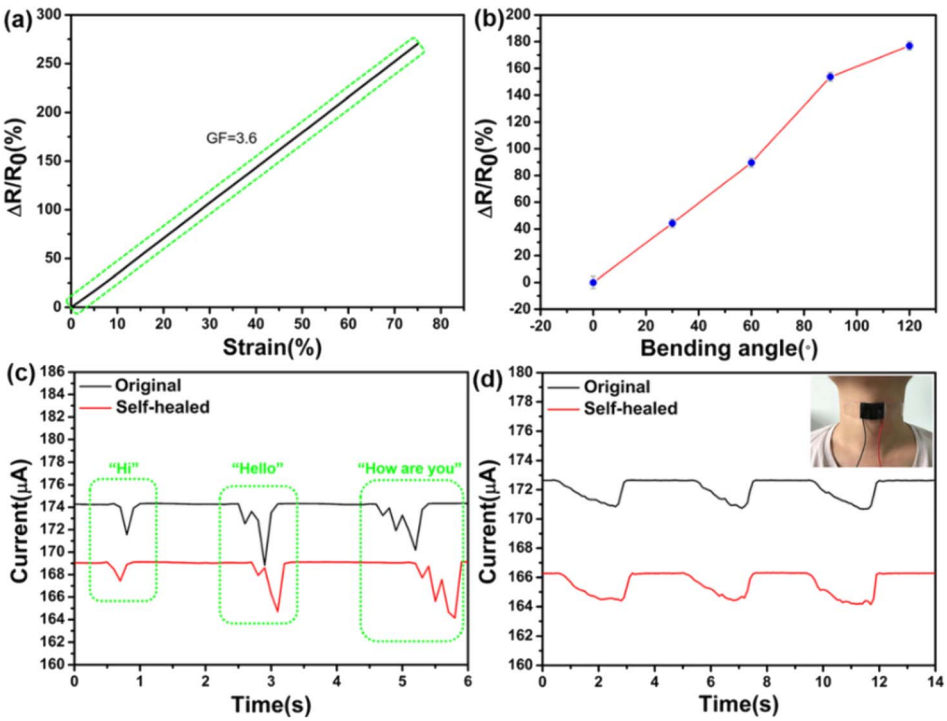

Fig. 25 (a) Relative resistance change of the MXene/PDMS flexible sensor during stretching; (b) relative resistance change of the MXene/PDMS flexible sensor when the elbow is bent; (c) current change of the MXene/PDMS flexible sensor when recognizing different words; (d) current change of the MXene/PDMS flexible sensor during swallowing[83] (Copyright 2020, The American Chemical Society).

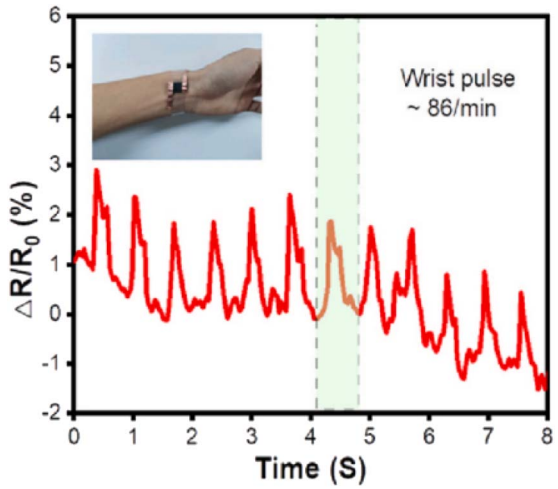

Fig. 26 Schematic diagram of human pulse monitoring by the CNT-MXene/PDMS flexible sensor[112] (Copyright 2022, Elsevier).

some flexible sensors with high sensitivity can also monitor small muscle movements such as swallowing, expression changes, and speaking.[128] Zhang[83] *et al.* prepared a self-healing MXene/PDMS flexible sensor through the esterification reaction and the Schiff base reaction. The sensor can not only monitor large-scale movement, but also monitor small muscle movement. The sensor is attached to the neck. According to the difference of vocal cord vibration when people read different words, different words can be accurately identified, as shown in Fig. 25.

6.2 Health management

Since the 21st century, with the continuous improvement of people's living standards, people's attention to physical health has gradually increased. Pulse and heartbeat are one of the important means to evaluate human health.[128,131,132] If the abnormality of heartbeat or pulse can be accurately monitored, people can seek medical advice in time to avoid risks. The current research shows that the piezoresistive flexible sensor can accurately monitor the heartbeat and pulse.[129,130] As mentioned above, Xu[112] *et al.* combined carbon nanotube (CNT) and MXene onto porous PDMS sponge and developed a multifunctional strain sensor with wide sensing range (105% strain), high sensitivity (GF = 1939), fast response (158 ms), and sufficient reliability under repeated stretching, compression, and bending cycles. Also, it can accurately monitor the pulse and heartbeat of the human body, as shown in Fig. 26.

7 Conclusion

In recent years, the attention of flexible sensors has become increasingly high. Polysiloxane materials have great application prospects in the preparation of piezoresistive flexible sensors due to their excellent human affinity, chemical resistance, mechanical properties, and other characteristics. This article summarizes the latest research progress of polysiloxane-based piezoresistive flexible sensors in recent years, including flexible matrix materials, conductive fillers, and preparation processes, and looks forward to their application fields.

Polysiloxane-based piezoresistive flexible sensors have rapidly developed due to their important role in human health management, motion monitoring, and other fields. However, there is still a gap in meeting practical needs for piezoresistive flexible sensors. For example, the hysteresis and nonlinear behavior of sensors always hinder their practical application, and the composite use of multiple conductive materials and novel preparation processes are possible ways to solve this problem. In addition, the relevant devices and technologies that support the use of piezoresistive flexible sensors in real life are not mature, such as portable power supply devices and wireless signal transmission devices. At present, there is still room for improvement in this area of research. At present, most flexible sensors are limited to a single signal response, and how to achieve multiple responses for flexible sensors is also one of the challenges that needs to be solved.

In summary, polysiloxane-based piezoresistive flexible sensors have broad application prospects and development potential, but the research on related supporting devices still needs to be improved, and the application feasibility also needs to be continuously broken through. We believe that polysiloxane-based piezoresistive flexible human electronic sensors can demonstrate enormous application potential in the fields of human motion detection, health management, wearable electronic devices, and electronic skin.

Conflicts of interest

There are no conflicts to declare.

Acknowledgements

This work was financially supported by Natural Science Foundation of Shandong Province (No. ZR2020LFG002); Jiangsu Graduate Research Innovation Program (No. Kycx22_3009); Jiangsu Graduate Practical Innovation Program (No. SjCX22_1331).

References

1 G. Shao, J. Jiang, M. Jiang, J. Su, W. Liu, H. Wang, H. Xu, H. Lit and R. Zhang, *J. Adv. Ceram.*, 2020, **9**, 374–379.
2 T. A. Blank, L. P. Eksperiandova and K. N. Belikov, *Sens. Actuators, B*, 2016, **228**, 416–442.
3 Y. Ermolenko, D. Kalyagin, I. Alekseev, E. Bychkov, V. Kolodnikov, N. Melnikova, I. Murin, Y. Mourzina and Y. Vlasov, *Sens. Actuators, B*, 2015, **207**, 940–944.
4 J.-Y. Kim, A. Mirzaei, J.-H. Kim, J.-H. Lee, H. W. Kim and S. S. Kim, *Sens. Actuators, B*, 2019, **296**, 126673.
5 K. Xu, Y. Lu and K. Takei, *Adv. Funct. Mater.*, 2020, **31**, 2007436.
6 Z. Ren, J. Yang, D. Qi, P. Sonar, L. Liu, Z. Lou, G. Shen and Z. Wei, *Adv. Mater. Technol.*, 2021, **6**, 2000889.

7 X. Chang, L. Chen, J. Chen, Y. Zhu and Z. Guo, *Adv. Compos. Hybrid Mater.*, 2021, **4**, 435–450.
8 Z. Liu, T. Zhu, J. Wang, Z. Zheng, Y. Li, J. Li and Y. Lai, *Nano-Micro Lett.*, 2022, **14**, 61.
9 K. Sakamoto, C. Tsujioka, M. Sasaki, T. Miyashita, M. Kitano and S. Kudo, *Gait Posture*, 2021, **86**, 180–185.
10 R. A. Bilodeau, A. Mohammadi Nasab, D. S. Shah and R. Kramer-Bottiglio, *Soft Matter*, 2020, **16**, 5827–5839.
11 J. Zeng, W. Ma, Q. Wang, S. Yu, M. T. Innocent, H. Xiang and M. Zhu, *Compos. Commun.*, 2021, **25**, 100735.
12 S. Raman and A. Ravi Sankar, *J. Mater. Sci.*, 2022, **57**, 13152–13178.
13 W. Wang, S. Yang, K. Ding, L. Jiao, J. Yan, W. Zhao, Y. Ma, T. Wang, B. Cheng and Y. Ni, *Chem. Eng. J.*, 2021, **425**, 129949.
14 X. X. Gong, G. T. Fei, W. B. Fu, M. Fang, X. D. Gao, B. N. Zhong and L. D. Zhang, *Org. Electron.*, 2017, **47**, 51–56.
15 A. Nag, R. B. V. B. Simorangkir, E. Valentin, T. Bjorninen, L. Ukkonen, R. M. Hashmi and S. C. Mukhopadhyay, *IEEE Access*, 2018, **6**, 71020–71027.
16 Y.-N. Kim, J. Lee and S.-K. Kang, *J. Mech. Sci. Technol.*, 2022, **36**, 1059–1077.
17 Y. Si, S. Chen, M. Li, S. Li, Y. Pei and X. Guo, *Adv. Intell. Syst.*, 2022, **4**, 2100046.
18 F. S. Irani, A. H. Shafaghi, M. C. Tasdelen, T. Delipinar, C. E. Kaya, G. G. Yapici and M. K. Yapici, *Micromachines*, 2022, **13**, 119.
19 S. Wu, J. Zhang, R. B. Ladani, A. R. Ravindran, A. P. Mouritz, A. J. Kinloch and C. H. Wang, *ACS Appl. Mater. Interfaces*, 2017, **9**, 14207–14215.
20 L. Wang, Y. Chen, L. Lin, H. Wang, X. Huang, H. Xue and J. Gao, *Chem. Eng. J.*, 2019, **362**, 89–98.
21 Y. Li, Y. A. Samad, T. Taha, G. Cai, S.-Y. Fu and K. Liao, *ACS Sustainable Chem. Eng.*, 2016, **4**, 4288–4295.
22 M. O. Tas, M. A. Baker, M. G. Masteghin, J. Bentz, K. Boxshall and V. Stolojan, *ACS Appl. Mater. Interfaces*, 2019, **11**, 39560–39573.
23 W. Wang, D. Chen, J. Liu, J. zhu, P. Zhang, L. Yang, H. Chen and Y. Wang, *J. Phys. D: Appl. Phys.*, 2020, **53**, 095405.
24 Z. Duan, Y. Jiang, Q. Huang, Q. Zhao, Z. Yuan, Y. Zhang, S. Wang, B. Liu and H. Tai, *J. Mater. Chem. C*, 2021, **9**, 14003–14011.
25 Z. Duan, Y. Jiang, Q. Huang, Z. Yuan, Q. Zhao, S. Wang, Y. Zhang and H. Tai, *J. Mater. Chem. C*, 2021, **9**, 13659–13667.
26 Z. Duan, Y. Jiang, Q. Huang, S. Wang, Y. Wang, H. Pan, Q. Zhao, G. Xie, X. Du and H. Tai, *Smart Mater. Struct.*, 2021, **30**, 055012.
27 Z. Duan, Y. Jiang, Q. Huang, S. Wang, Q. Zhao, Y. Zhang, B. Liu, Z. Yuan, Y. Wang and H. Tai, *Cellulose*, 2021, **28**, 6389–6402.
28 H. Tai, Z. Duan, Y. Wang, S. Wang and Y. Jiang, *ACS Appl. Mater. Interfaces*, 2020, **12**, 31037–31053.
29 Z. Duan, Y. Jiang, S. Wang, Z. Yuan, Q. Zhao, G. Xie, X. Du and H. Tai, *ACS Sustain. Chem. Eng.*, 2019, **7**, 17474–17481.
30 S. K. Hong, S. Yang, S. J. Cho, H. Jeon and G. Lim, *Sensors*, 2018, **18**, 1171.
31 S. Han Min, A. M. Asrulnizam, M. Atsunori and M. Mariatti, *Mater. Today: Proc.*, 2019, **17**, 616–622.
32 S. Wu, S. Peng and C. H. Wang, *Sens. Actuators, A*, 2018, **279**, 90–100.
33 L. Liu, Q. Zhang, D. Zhao, A. Jian, J. Ji, Q. Duan, W. Zhang and S. Sang, *J. Sens.*, 2017, **2017**, 1–8.
34 H. Niu, H. Zhou, H. Wang and T. Lin, *Macromol. Mater. Eng.*, 2016, **301**, 707–713.
35 Y. Zheng, Y. Li, Z. Li, Y. Wang, K. Dai, G. Zheng, C. Liu and C. Shen, *Compos. Sci. Technol.*, 2017, **139**, 64–73.
36 S. Wang, P. Xiao, Y. Liang, J. Zhang, Y. Huang, S. Wu, S.-W. Kuo and T. Chen, *J. Mater. Chem. C*, 2018, **6**, 5140–5147.
37 J. Lee, M. Lim, J. Yoon, M. S. Kim, B. Choi, D. M. Kim, D. H. Kim, I. Park and S. J. Choi, *ACS Appl. Mater. Interfaces*, 2017, **9**, 26279–26285.
38 X. Wang, J. Li, H. Song, H. Huang and J. Gou, *ACS Appl. Mater. Interfaces*, 2018, **10**, 7371–7380.
39 J. Li, S. Zhao, X. Zeng, W. Huang, Z. Gong, G. Zhang, R. Sun and C. P. Wong, *ACS Appl. Mater. Interfaces*, 2016, **8**, 18954–18961.
40 M. K. Filippidou, E. Tegou, V. Tsouti and S. Chatzandroulis, *Microelectron. Eng.*, 2015, **142**, 7–11.
41 Y. Chen, L. Wang, Z. Wu, J. Luo, B. Li, X. Huang, H. Xue and J. Gao, *Composites, Part B*, 2019, **176**, 107358.
42 S. Shengbo, L. Lihua, J. Aoqun, D. Qianqian, J. Jianlong, Z. Qiang and Z. Wendong, *Nanotechnology*, 2018, **29**, 255202.
43 Y. Q. Li, P. Huang, W. B. Zhu, S. Y. Fu, N. Hu and K. Liao, *Sci. Rep.*, 2017, **7**, 45013.
44 I. Kim, K. Woo, Z. Zhong, P. Ko, Y. Jang, M. Jung, J. Jo, S. Kwon, S. H. Lee, S. Lee, H. Youn and J. Moon, *Nanoscale*, 2018, **10**, 7890–7897.
45 Y. Hu, T. Zhao, P. Zhu, Y. Zhang, X. Liang, R. Sun and C.-P. Wong, *Nano Res.*, 2018, **11**, 1938–1955.
46 M. Nankali, N. M. Nouri, N. Geran Malek and M. A. Sanjari Shahrezaei, *J. Compos. Mater.*, 2019, **53**, 3047–3060.
47 X. Zhou, L. Zhu, L. Fan, H. Deng and Q. Fu, *ACS Appl. Mater. Interfaces*, 2018, **10**, 31655–31663.
48 S. Zhang, H. Zhang, G. Yao, F. Liao, M. Gao, Z. Huang, K. Li and Y. Lin, *J. Alloys Compd.*, 2015, **652**, 48–54.
49 K. Liu, C. Yang, L. Song, Y. Wang, Q. Wei, Alamusi, Q. Deng and N. Hu, *Compos. Sci. Technol.*, 2022, **218**, 109148.
50 Y. Zheng, Y. Li, K. Dai, Y. Wang, G. Zheng, C. Liu and C. Shen, *Compos. Sci. Technol.*, 2018, **156**, 276–286.
51 Q. Zheng, X. Liu, H. Xu, M. S. Cheung, Y. W. Choi, H. C. Huang, H. Y. Lei, X. Shen, Z. Wang, Y. Wu, S. Y. Kim and J. K. Kim, *Nanoscale Horiz.*, 2018, **3**, 35–44.
52 Y. Wang, T. Yang, J. Lao, R. Zhang, Y. Zhang, M. Zhu, X. Li, X. Zang, K. Wang, W. Yu, H. Jin, L. Wang and H. Zhu, *Nano Res.*, 2015, **8**, 1627–1636.
53 X. M. Zhang, X. L. Yang and K. Y. Wang, *J. Mater. Sci.: Mater. Electron.*, 2019, **30**, 19319–19324.
54 D. Guo, X. Pan and H. He, *Sens. Actuators, A*, 2019, **298**, 111608.
55 G. Li, K. Dai, M. Ren, Y. Wang, G. Zheng, C. Liu and C. Shen, *J. Mater. Chem. C*, 2018, **6**, 6575–6583.

56 F. Zhang, S. Wu, S. Peng, Z. Sha and C. H. Wang, *Compos. Sci. Technol.*, 2019, **172**, 7–16.
57 M. Amjadi, K.-U. Kyung, I. Park and M. Sitti, *Adv. Funct. Mater.*, 2016, **26**, 1678–1698.
58 Y. Gao, X. Fang, J. Tan, T. Lu, L. Pan and F. Xuan, *Nanotechnology*, 2018, **29**, 235501.
59 W. Li, Y. He, J. Xu, W.-y. Wang, Z.-t. Zhu and H. Liu, *J. Alloy Compd.*, 2019, **803**, 332–340.
60 X. Liao, Z. Zhang, Z. Kang, F. Gao, Q. Liao and Y. Zhang, *Mater. Horiz.*, 2017, **4**, 502–510.
61 Y. Pang, H. Tian, L. Tao, Y. Li, X. Wang, N. Deng, Y. Yang and T. L. Ren, *ACS Appl. Mater. Interfaces*, 2016, **8**, 26458–26462.
62 X. Liu, D. Liu, J. H. Lee, Q. Zheng, X. Du, X. Zhang, H. Xu, Z. Wang, Y. Wu, X. Shen, J. Cui, Y. W. Mai and J. K. Kim, *ACS Appl. Mater. Interfaces*, 2019, **11**, 2282–2294.
63 W. Hu, S. Chen, B. Zhuo, Q. Li, R. Wang and X. Guo, *IEEE Electron Device Lett.*, 2016, **37**, 667–670.
64 D. Y. Wang, L. Q. Tao, Y. Liu, T. Y. Zhang, Y. Pang, Q. Wang, S. Jiang, Y. Yang and T. L. Ren, *Nanoscale*, 2016, **8**, 20090–20095.
65 S. H. Jeong, S. Zhang, K. Hjort, J. Hilborn and Z. Wu, *Adv. Mater.*, 2016, **28**, 5830–5836.
66 S. Yao, X. Nie, X. Yu, B. Song and J. Blecke, *IEEE Sens. Lett.*, 2017, **1**, 1–4.
67 J. Ma, P. Wang, H. Chen, S. Bao, W. Chen and H. Lu, *ACS Appl. Mater. Interfaces*, 2019, **11**, 8527–8536.
68 J. Luan, Q. Wang, X. Zheng, Y. Li and N. Wang, *Micromachines*, 2019, **10**, 372.
69 D. Zhao, Q. Zhang, Y. Liu, Y. Zhang, X. Guo, Z. Yuan, W. Zhang, R. Zhang, J. W. Lian and S. Sang, *Appl. Nanosci.*, 2019, **9**, 1469–1478.
70 X. Yan, C. R. Bowen, C. Yuan, Z. Hao and M. Pan, *Soft Matter*, 2019, **15**, 8001–8011.
71 A. S. Dahiya, J. Thireau, J. Boudaden, S. Lal, U. Gulzar, Y. Zhang, T. Gil, N. Azemard, P. Ramm, T. Kiessling, C. O'Murchu, F. Sebelius, J. Tilly, C. Glynn, S. Geary, C. O'Dwyer, K. M. Razeeb, A. Lacampagne, B. Charlot and A. Todri-Sanial, *J. Electrochem. Soc.*, 2019, **167**, 037516.
72 T. Sakorikar, M. K. Kavitha, P. Vayalamkuzhi and M. Jaiswal, *Sci. Rep.*, 2017, **7**, 2598.
73 Z. Yang, Z. Wu, D. Jiang, R. Wei, X. Mai, D. Pan, S. Vupputuri, L. Weng, N. Naik and Z. Guo, *J. Mater. Chem. C*, 2021, **9**, 2752–2762.
74 N. Hu, Y. Karube, C. Yan, Z. Masuda and H. Fukunaga, *Acta Mater.*, 2008, **56**, 2929–2936.
75 Q. Yu, R. Ge, J. Wen, T. Du, J. Zhai, S. Liu, L. Wang and Y. Qin, *Nat. Commun.*, 2022, **13**, 778.
76 J. Lee, S. Pyo, D. S. Kwon, E. Jo, W. Kim and J. Kim, *Small*, 2019, **15**, e1805120.
77 H. Souri, H. Banerjee, A. Jusufi, N. Radacsi, A. A. Stokes, I. Park, M. Sitti and M. Amjadi, *Adv. Intell. Syst.*, 2020, **2**, 2000039.
78 C. Jin, D. Liu, M. Li and Y. Wang, *J. Mater. Sci.: Mater. Electron.*, 2020, **31**, 4788–4796.
79 S. J. Paul, I. Elizabeth and B. K. Gupta, *ACS Appl. Mater. Interfaces*, 2021, **13**, 8871–8879.
80 D. Song, X. Li, X. P. Li, X. Jia, P. Min and Z. Z. Yu, *J. Colloid Interface Sci.*, 2019, **555**, 751–758.
81 Y. Shan, Z. Li, T. Yu, X. Wang, H. N. Cui, K. Yang and Y. Cui, *Compos. Sci. Technol.*, 2022, **218**, 109208.
82 M. Tang, Z. Li, K. Wang, Y. Jiang, M. Tian, Y. Qin, Y. Gong, Z. Li and L. Wu, *J. Mater. Chem. A*, 2022, **10**, 1750–1759.
83 K. Zhang, J. Sun, J. Song, C. Gao, Z. Wang, C. Song, Y. Wu and Y. Liu, *ACS Appl. Mater. Interfaces*, 2020, **12**, 45306–45314.
84 K. Zhang, J. Zhang, Y. Liu, Z. Wang, C. Yan, C. Song, C. Gao and Y. Wu, *J. Colloid Interface Sci.*, 2021, **599**, 360–369.
85 F. Yin, H. Lu, H. Pan, H. Ji, S. Pei, H. Liu, J. Huang, J. Gu, M. Li and J. Wei, *Sci. Rep.*, 2019, **9**, 2403.
86 W.-W. Kong, C.-G. Zhou, K. Dai, L.-C. Jia, D.-X. Yan and Z.-M. Li, *Composites, Part B*, 2021, **225**, 109275.
87 H. Liu, Q. Li, S. Zhang, R. Yin, X. Liu, Y. He, K. Dai, C. Shan, J. Guo, C. Liu, C. Shen, X. Wang, N. Wang, Z. Wang, R. Wei and Z. Guo, *J. Mater. Chem. C*, 2018, **6**, 12121–12141.
88 D. Wang, X. Zhou, R. Song, Z. Wang, C. Fang, N. Li, C. Wang, J. Deng and Y. Huang, *Int. J. Biol. Macromol.*, 2021, **181**, 160–168.
89 S. Zheng, Y. Jiang, X. Wu, Z. Xu, Z. Liu, W. Yang and M. Yang, *Compos. Sci. Technol.*, 2021, **201**, 108546.
90 Y. Jiang, Y. Chen, W. Wang and D. Yu, *Colloids Surf., A*, 2021, **629**, 127477.
91 O. Kanoun, A. Bouhamed, R. Ramalingame, J. R. Bautista-Quijano, D. Rajendran and A. Al-Hamry, *Sensors*, 2021, **21**, 341.
92 T. Yan, Y. Wu, W. Yi and Z. Pan, *Sens. Actuators, A*, 2021, **327**, 112755.
93 S. Zhu, H. Sun, Y. Lu, S. Wang, Y. Yue, X. Xu, C. Mei, H. Xiao, Q. Fu and J. Han, *ACS Appl. Mater. Interfaces*, 2021, **13**, 59142–59153.
94 Y. Wang, F. Wang, S. Yazigi, D. Zhang, X. Gui, Y. Qi, J. Zhong and L. Sun, *Carbon*, 2021, **173**, 849–856.
95 K. Zhang, Z. Wang, Y. Liu, H. Zhao, C. Gao and Y. Wu, *Chin. J. Polym. Sci.*, 2022, **40**, 384–393.
96 A. Mehmood, N. M. Mubarak, M. Khalid, R. Walvekar, E. C. Abdullah, M. T. H. Siddiqui, H. A. Baloch, S. Nizamuddin and S. Mazari, *J. Environ. Chem. Eng.*, 2020, **8**, 103743.
97 Y. He, D. Wu, M. Zhou, Y. Zheng, T. Wang, C. Lu, L. Zhang, H. Liu and C. Liu, *ACS Appl. Mater. Interfaces*, 2021, **13**, 15572–15583.
98 S. Niu, X. Chang, Z. Zhu, Z. Qin, J. Li, Y. Jiang, D. Wang, C. Yang, Y. Gao and S. Sun, *ACS Appl. Mater. Interfaces*, 2021, **13**, 55307–55318.
99 M. Iqra, F. Anwar, R. Jan and M. A. Mohammad, *Sci. Rep.*, 2022, **12**, 4882.
100 U. Pierre Claver and G. Zhao, *Adv. Eng. Mater.*, 2021, **23**, 2001187.
101 Z. Duan, Z. Yuan, Y. Jiang, L. Yuan and H. Tai, *J. Mater. Chem. C*, 2023, **11**, 5585–5600.
102 M. Li, Y. Pei, Y. Cao, S. Chen and X. Guo, *Flexible Printed Electron.*, 2021, **6**, 043002.
103 R. Li, Q. Zhou, Y. Bi, S. Cao, X. Xia, A. Yang, S. Li and X. Xiao, *Sens. Actuators, A*, 2021, **321**, 112425.

104 S. Li, R. Xu, J. Wang, Y. Yang, Q. Fu and C. Pan, *J. Colloid Interface Sci.*, 2022, **617**, 372–382.
105 Q. Xia, S. Wang, W. Zhai, C. Shao, L. Xu, D. Yan, N. Yang, K. Dai, C. Liu and C. Shen, *Compos. Commun.*, 2021, **26**, 100809.
106 M. Hu, Y. Gao, Y. Jiang, H. Zeng, S. Zeng, M. Zhu, G. Xu and L. Sun, *Adv. Compos. Hybrid Mater.*, 2021, **4**, 514–520.
107 C. Ma, M. G. Ma, C. Si, X. X. Ji and P. Wan, *Adv. Funct. Mater.*, 2021, **31**, 2009524.
108 H. Riazi, G. Taghizadeh and M. Soroush, *ACS Omega*, 2021, **6**, 11103–11112.
109 Y. Pei, X. Zhang, Z. Hui, J. Zhou, X. Huang, G. Sun and W. Huang, *ACS Nano*, 2021, **15**, 3996–4017.
110 J. Luo, S. Gao, H. Luo, L. Wang, X. Huang, Z. Guo, X. Lai, L. Lin, R. K. Y. Li and J. Gao, *Chem. Eng. J.*, 2021, **406**, 126898.
111 Z. Zhang, L. Weng, K. Guo, L. Guan, X. Wang and Z. Wu, *Ceram. Int.*, 2022, **48**, 4977–4985.
112 B. Xu, F. Ye, R. Chen, X. Luo, G. Chang and R. Li, *Ceram. Int.*, 2022, **48**, 10220–10226.
113 C. Chen, F. Chu, Y. Zhang, M. Ma, R. Sun, P. Jia and J. Sun, *ACS Appl. Electron. Mater.*, 2023, **5**, 1429–1436.
114 D. Jiang, Y. Wang, B. Li, C. Sun, Z. Wu, H. Yan, L. Xing, S. Qi, Y. Li, H. Liu, W. Xie, X. Wang, T. Ding and Z. Guo, *Macromol. Mater. Eng.*, 2019, **304**, 1900074.
115 J. Chen, Y. Zhu and W. Jiang, *Compos. Sci. Technol.*, 2020, **186**, 107938.
116 X. Liu, X. Liang, Z. Lin, Z. Lei, Y. Xiong, Y. Hu, P. Zhu, R. Sun and C. P. Wong, *ACS Appl. Mater. Interfaces*, 2020, **12**, 42420–42429.
117 X. Xu, Y. Chen, P. He, S. Wang, K. Ling, L. Liu, P. Lei, X. Huang, H. Zhao, J. Cao and J. Yang, *Nano Res.*, 2021, **14**, 2875–2883.
118 Y.-F. Chen, J. Li, Y.-J. Tan, J.-H. Cai, X.-H. Tang, J.-H. Liu and M. Wang, *Compos. Sci. Technol.*, 2019, **177**, 41–48.
119 J. Du. Qilu University of Technology, 2020.
120 J. Chen, J. Zheng, Q. Gao, J. Zhang, J. Zhang, O. Omisore, L. Wang and H. Li, *Appl. Sci.*, 2018, **8**, 345.
121 S. Zheng, X. Wu, Y. Huang, Z. Xu, W. Yang, Z. Liu, S. Huang, B. Xie and M. Yang, *Composites, Part A*, 2019, **121**, 510–516.
122 J. Park, Y. Lee, J. Hong, Y. Lee, M. Ha, Y. Jung, H. Lim, S. Y. Kim and H. Ko, *ACS Nano*, 2014, **8**, 12020–12029.
123 H. H. Chou, A. Nguyen, A. Chortos, J. W. To, C. Lu, J. Mei, T. Kurosawa, W. G. Bae, J. B. Tok and Z. Bao, *Nat. Commun.*, 2015, **6**, 8011.
124 X. Wang, Y. Gu, Z. Xiong, Z. Cui and T. Zhang, *Adv. Mater.*, 2014, **26**, 1336–1342.
125 X. Zhou, Z. Gong, J. Fan and Y. Chen, *Polymer*, 2021, **237**, 124357.
126 Z. Ma, H. Li, X. Jing, Y. Liu and H.-Y. Mi, *Sens. Actuators, A*, 2021, **329**, 112800.
127 D. Qi, K. Zhang, G. Tian, B. Jiang and Y. Huang, *Adv. Mater.*, 2021, **33**, 2003155.
128 Y. Lu, M. C. Biswas, Z. Guo, J. W. Jeon and E. K. Wujcik, *Biosens. Bioelectron.*, 2019, **123**, 167–177.
129 Y. Li, Y. Liu, S. R. A. Bhuiyan, Y. Zhu and S. Yao, *Small Struct.*, 2021, **3**, 2100131.
130 X. Liu, J. Miao, Q. Fan, W. Zhang, X. Zuo, M. Tian, S. Zhu, X. Zhang and L. Qu, *Adv. Fiber Mater.*, 2022, **4**, 571.
131 N. Yuan, C. Wang, J. Ji and K. Zhou, *J. Mater. Sci-Mate. El.*, 2021, **32**, 27656–27665.
132 R. Luo, Y. Cui, H. Li, Y. Wu, B. Du, S. Zhou and J. Hu, *ACS Appl. Nano Mater.*, 2023, **6**, 7065–7076.
133 S. Zhu, Z. Lei, Y. Dou, C.-W. Lou, J.-H. Lin and J. Li, *Chem. Eng. J.*, 2023, **452**, 139403.
134 J. Li, Y. Feng, W. Chen, S. Zhang, J. Ma, S. Chen, S. Liu, C. Cao and Y. Zhang, *Prog. Mater. Sci.*, 2023, **132**, 101045.